Noise Detection Based Adaptive Control of Dual Staged Grid Interfaced PV System

Pragnyashree Ray
Dept. of Electrical Engineering
National Institute of Technology
Rourkela, India
pragnya.sangram@gmail.com

Pravat Kumar Ray
Dept. of Electrical Engineering
National Institute of Technology
Rourkela, India
rayp@nitrkl.ac.in

Bhanu Pratap Behera
Dept. of Electrical Engineering
National Institute of Technology
Rourkela, India
beherab@nitrkl.ac.in

Naresh Singh
Dept. of Electrical Engineering
National Institute of Technology
Rourkela, India
singh.naresh.ee@gmail.com

***Abstract*—Here, an adaptive controller is designed for a grid integrated photovoltaic (PV) system. The PV voltage is continually monitored and regulated by the boost converter by tracking maximum power point. The proposed control scheme employs noise detection-based technique for active power filtering (APF) along with its basic function of power management. It addresses various issues of a grid interconnected PV system such as reduction of grid current harmonics, regulation of DC-link voltage etc. besides managing power distribution between grid, load and PV system. This strategy is used to generate reference signals for controlling the grid interfaced PV voltage source inverter (VSI). Also, the behavior of the controller is observed under changing solar insolation and unbalanced load condition. Simplicity in structure, faster convergence rate, frequency adaptive detection and better steady state behaviour are the key features of the noise detection-based controller. Further, the performance of the controller is executed and studied with the help of simulation in MATLAB/Simulink and investigated by implementing this to experimental prototype of the presented system.**

Keywords—Adaptive control, current harmonics, DC-link voltage, grid, noise detection, PV, solar insolation.

I. INTRODUCTION

Increased dependency on the power electronic based devices has highly encouraged the involvement of non-linear loads and renewable energy based sources into the distribution system leading to deteriorated quality of power at the consumer end. So, it is a prime time to address the power quality challenges such as disturbance in the voltage at PCC, current harmonics, power loss etc. arising in the power distribution network. Therefore, there is need to make the optimal use of the grid interfaced PV inverter to render multiple service of alleviating power quality problems and managing power between grid, PV and load. To competently perform the aforesaid functions the design of the controller for the system must be efficient enough with respect to speed, accuracy, simplicity and robustness. There are so many control techniques reported which are used to eliminate current harmonics from grid current [1]. Akagi, Kanazawa and Nabae proposed a current compensation technique called Instantaneous Reactive Power Theory (IRPT), or commonly known as "p-q Theory" [2] in 1983. The p-q theory is based on alpha-beta transformation ($\alpha\beta\gamma$), also known as Clarke transformation. The IRPT can easily be implemented with power electronics-based shunt active filter for eliminating current harmonics [3]- [4].

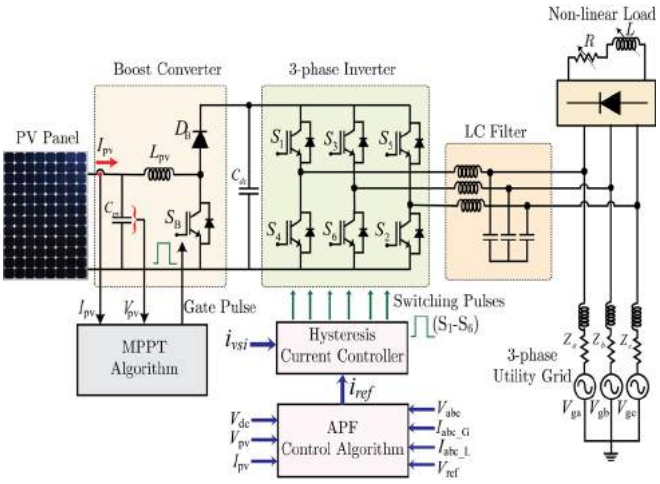

Fig. 1. System configuration

However, the performance of this controller is not good enough in case of unbalanced or distorted three phase system. The direct-quadrature-zero (DQZ) transformation known as “d-q theory” was brought by Robert H. Park in 1929 which was a combination of Clarke transform and the Park transform [5]. In SRF based method, Clarke transformation can be used to transform three phase abc to alpha-beta stationary reference frame and then it rotates the reference frame of ac waveform such that it become dc signal. After performing some control laws, the output ac quantities can be recovered by applying inverse transformation of d-q transform [6]. A double stage PV connected grid system [7] can be controlled by “d-q” control algorithm. A proportional resonant based current controller with multiple harmonics control in rotating frame have been discussed in [8]. Two proportional integral (PI) controllers for compensating both positive and negative sequences can be replaced by a proportional resonant [9]- [10] controller in a stationary frame. For a PV connected grid system, a decoupled adaptive noise detection (DAND) scheme is presented in which active power consumed by all three phases are detected separately [11]-[12]. An adaptive dc link voltage control model for varying PCC voltage in three phase grid tied PV system have been studied in [13]. This method reduces switching loss and increases the efficiency of VSI. An improved linear sinusoidal tracer (ILST) based on adaptive control theory is studied in [14] [15] which is very effective for compensation of harmonics present in current, compensation of reactive power, better voltage regulation under linear/non-linear loads.

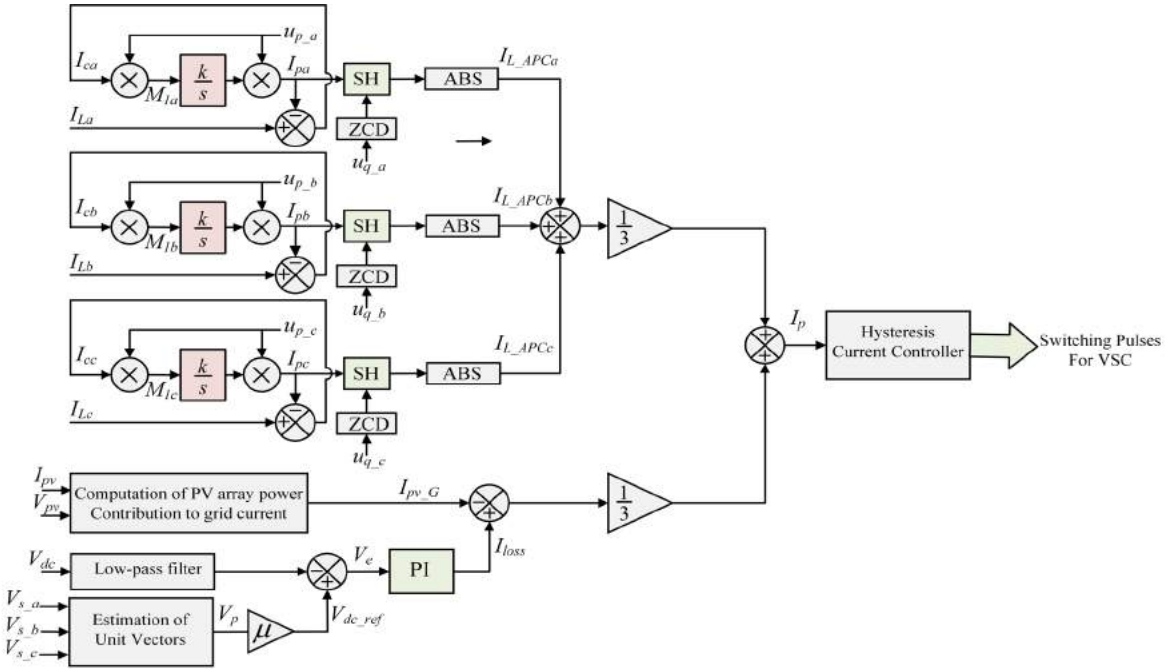

Fig. 2. Block diagram of noise detection-based control algorithm

In the presented work, the control of grid interfaced dual staged PV system is studied using an adaptive control based on noise detection technique to facilitate the multiple function of power quality betterment and power management. The structure of the paper is presented as: section II explicates the configuration of the system and its design. Section III illustrates regarding execution of control approach. The proposed controller is analysed utilising MATLAB/Simulink section IV and section V provides the conclusion of the presented work.

II. System Architecture

The architecture of the presented work is depicted in Fig. 1. The proposed system is composed of a dual staged PV (i.e., PV is interconnected to the grid interfaced voltage source inverter through a boost converter) connected to the grid and rectifier based load. The boost converter output and input of the voltage source Inverter (VSI) is connected through an interconnected capacitor C_{dc} which is called dc link capacitor. The ac side of the VSI is connected to point of common coupling (PCC) for current harmonic compensation through coupling inductors.

III. Control Approach

Here, a dual stage control approach is implemented to perform multiple operation of power handling and active power filtering of the system. First stage deals with maximum power extraction from solar PV array using MPPT controller combined with a boost converter and later stage includes estimation of reference current for VSI control, based on noise detection method. The main target of this controller is to eliminate noise and determine the fundamental part of load currents for each of the phases. The PV array contributes the necessary power to the grid by a voltage source inverter (VSI). The control algorithm is designed such a way that the grid can able to provide harmonic free current to the load under varied erratic circumstances such as changing solar insolation and unbalanced load condition.

A. Maximum Power Point Tracking (MPPT)

Perturb and Observe (P&O) algorithm based MPPT controller is used to achieve maximum power from a PV array [15].

B. Refrence Current Estimation

The steps involved for reference current generation for the switching of VSI using the presented technique is shown in Fig. 2. The controlled pulse to the VSI ensures elimination of grid current harmonics and provides sinusoidal three phase balanced grid current at PCC, even for an unbalanced non-linear load. The basic control approach of this algorithm is to determine the phase locking unit vectors, which is done by using PCC voltages. The every sample of PCC voltage is used to calculate the peak value for that particular time instant. The mathematical equation for peak value is given as:

$$V_p = \sqrt{\frac{2*(V_{s\_a}^2 + V_{s\_b}^2 + V_{s\_c}^2)}{3}} \quad (1)$$

where, V_{s_a} , V_{s_b} , V_{s_c} are the 3-phase voltage sensed from PCC terminal. The phase locking unit vectors for phase a, b, c are u_{p_a} , u_{p_b}, u_{p_c} respectviely, and that is determined as:

$$u_{p\_a} = \frac{V_{s\_a}}{V_p}, \quad u_{p\_b} = \frac{V_{s\_b}}{V_p}, \quad u_{p\_c} = \frac{V_{s\_c}}{V_p} \quad (2)$$

The quadrature unit sinusoids can be evaluated from in-phase synchronize sinusoids. The equation for three phase is given as follows:

$$u_{q\_a} = -\frac{(u_{p\_a})}{\sqrt{3}} + \frac{(u_{p\_c})}{\sqrt{3}} \quad (3)$$

$$u_{q\_b} = \frac{(\sqrt{3} * u_{p\_a})}{2} + \frac{(u_{p\_b} - u_{p\_c})}{2\sqrt{3}} \quad (4)$$

$$u_{q\_c} = -\frac{\sqrt{3} * u_{p\_a}}{2} + \frac{(u_{p\_b} - u_{p\_c})}{2\sqrt{3}} \quad (5)$$

The fundamental load current component is detected by eliminating noise from the signal for determination of active power drained by the load for each phase. The load currents and corresponding unit vectors gives input signals for noise cancellation, and depending on true power consumption of load, the line frequency component of load current is evaluated. The input load currents are compared with output of the noise detection block to calculate error component, which are projection of fundamental load current on the respective unit vector. These errors are multiplied by corresponding in-phase unit vectors, which give M_{1a}, M_{1b} and M_{1c} for phase a, b, c respectively. An integrator is used to sum up those product terms which are further multiplied by corresponding unit vectors to get output of noise detection block. The speed of this system is governed by the value of an internal parameter k. Speed of convergence can be increased by taking a high value of k, but it also increases steady state oscillations. Therefore, choosing the value is important for achieving good convergence rate as well as to minimize the steady state oscillation. A zero-crossing detector (ZCD) block is employed to track number of zero crossing of quadrature unit component. The sampling and hold (SH) block samples the fundamental part of load current at every zero crossing of quadrature unit component. The absolute value of sampling and hold block employed per phase, provides the active power for load which is summed up to get total load power. The key benefit of this algorithm is that it can adjust power load consumption with the change in load and grid frequency.

The contribution of PV array to the grid can be estimated by considering PV power and PCC voltage. The PV power is calculated by MPPT algorithm and current contribution to the grid is given as:

$$I_{pv\_g} = \frac{2 * (I_{pv} V_{pv})}{3 * V_p} \quad (6)$$

The dc link voltage has to be maintained for efficient performance of VSI. For that purpose, dc link voltage needs to be adjusted adaptively with respect to the PCC voltage. Calculation of reference voltage across dc-link is given as:

$$V_{dc\_ref} = \mu * (\sqrt{3} * V_{peak\_line}) \quad (7)$$

where, $\mu > 1$. Practically, a voltage drop can be seen across switches and interfacing inductors. So, the value of μ need to be such that, the dc link voltage always remains higher than PCC voltage. For that purpose, here we take $\mu = 1.1$.

A low pass filter (LPF) is introduced to eradicate oscillating part from dc link voltage which is compared with the reference dc link voltage to calculate error between reference and actual value of dc link voltage. The error is then passes through a PI controller for estimating the loss component which is one of the main part of grid current. Considering the steady state condition, the loss equation is given as:

$$I_{loss}(k) = I_{loss}(k-1) + k_p * [V_e(k) - V_e(k-1)] + k_i * V_e(k) \quad (8)$$

Where, I_{loss} is loss component current contributing to grid current, v_e is Dc link error voltage, K_p is Proportional constant, K_i is Integral constant. The magnitude of balanced reference grid current is evaluated by given equation.

$$I_p = \frac{(\sum_{j=a,b,c} I_{L\_APC_j} + I_{loss} - I_{pv\_g})}{3} \quad (9)$$

where, I_{L_APC} is active power requirement of the load. The switching logic for VSI operation is controlled through a hysteresis current controller (HCC). The generation of signals for switching through HCC is shown in Fig. 3. After multiplication of balanced reference grid current with corresponding unit vector, it is compared with the grid

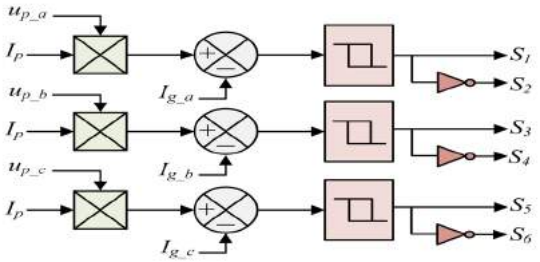

Fig. 3. Block diagram of hysteresis current controller

phase current and then pulse is generated using those reference current signals. Reference currents for each phase is given as:

$$I_{g\_a\_ref} = I_p * u_{p\_a} \quad (10)$$

$$I_{g\_b\_ref} = I_p * u_{p\_b} \quad (11)$$

$$I_{g\_c\_ref} = I_p * u_{p\_c} \quad (12)$$

C. Design of DC- Link Capacitor

Depending upon voltage fluctuation for case of transient or unbalanced load, the DC link capacitor is selected. Using the energy conservation principle, the DC link capacitor C_{dc} is calculated [6].

$$\frac{1}{2} C_{dc} \left[V_{dcnom}^2 - V_{dcmin}^2 \right] = 3 * (V_{ph} * a * I_{ph}) * t \quad (13)$$

$$C_{dc} = \frac{6V * a * I_{ph} * t}{V_{dcnom}^2 - V_{dcmin}^2} \quad (14)$$

where, V_{dcnom} is the dc-link voltage at normal condition, V_{dcmin} is minimum voltage across the dc-link capacitor, a is

overloading factor, V_{ph} is phase voltage, I_{ph} is phase current of VSI, and t is the time taken by the dc link voltage to recover.

D. Design of Interfacing Inductor of VSI

The VSI cannot be connected directly to the grid as in such cases a huge current will flow in either direction that may damage the components. So, for the safety purpose an inductor is used as an impedance. The inductor also eliminates high frequency components of the current, therefore, interfacing inductor (L_f) need to be designed properly. The following relation is used to choose the inductor value [6] -

$$L_f = \frac{\sqrt{3} * m_i * V_{dc}}{12 * a * f_s * D_i} \qquad (15)$$

where, m_i is modulation index (approximately 1), V_{dc} is dc-link voltage, a is overload factor (assumed 1.2), f_s is switching frequency, Δ_i is the ripple current (assume 5% of VSI current).

IV. Results and Discussions

A. Simulation Result

The presented work is executed in MATLAB/Simulink. The parameters required for simulating the model are mentioned in Table I.

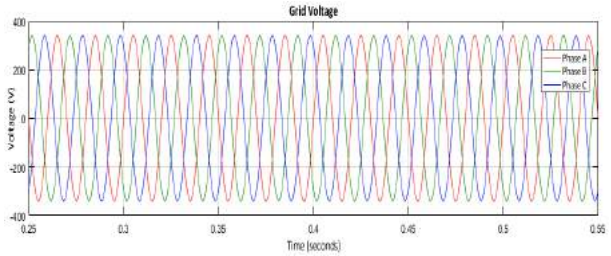

Fig. 4. Grid voltage Vs time

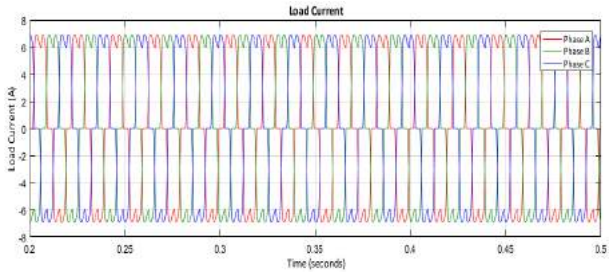

Fig. 5(a). Load current Vs time

Grid current and voltage plots are presented in Fig. 4 and 5(a) respectively. From Fig. 5(a), it is seen that due to non-linear load the grid current is distorted. From FFT analysis, THD of load current is found to be 19.35% as in Fig. 5(b).

The behaviour of the controller is investigated at 25°C and different solar insolation. The operation of the MPPT algorithm is verified by analysing PV voltage and PV power plot. From Fig. 6(a), it is seen that initially irradiance is 1000 W/m^2 which is reduced to 800 W/m^2 at t = 0.3 sec.

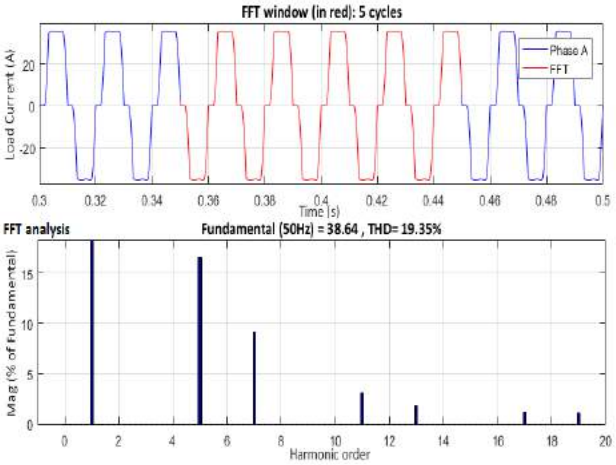

Fig. 5(b). THD of load current

The variation of PV voltage at different irradiances, is displayed in Fig. 6(b). It is followed that the PV voltage is around 726 V at 1000 W/m^2 and with the sudden change in irradiance at 0.3 second the PV voltage also falls. At 800 W/m^2 the PV voltage is around 680 V.

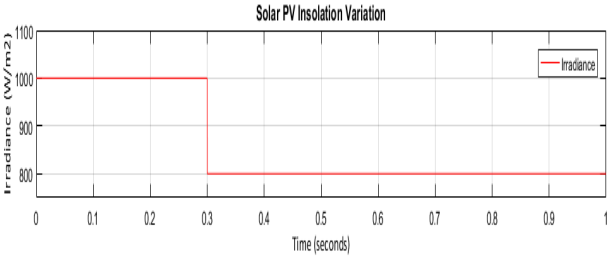

Fig. 6(a). Varying solar irradiance

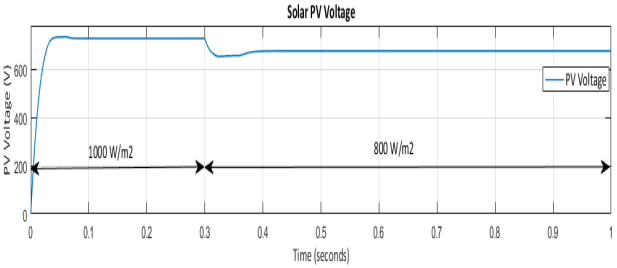

Fig. 6(b). PV voltage w.r.t to varying solar irradiance

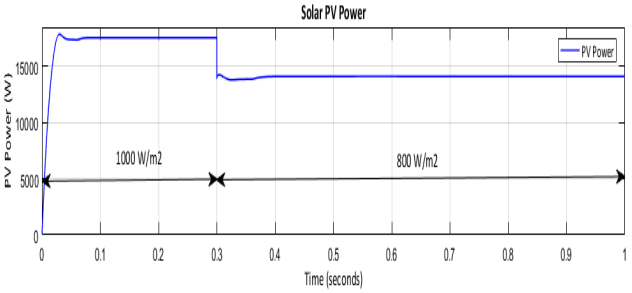

Fig. 6(c). PV power w.r.t to varying solar irradiance

The P&O based MPPT controller helps to track maximum power, even at sudden change in irradiance. Fig. 6(c) shows that 17.5 KW power is extracted at 1000 W/m^2 from PV solar. When the irradiance changes to 800 W/m^2, PV provides 14.2 KW power. Hence, the MPPT controller provides enough control to extract maximum power at different irradiances.

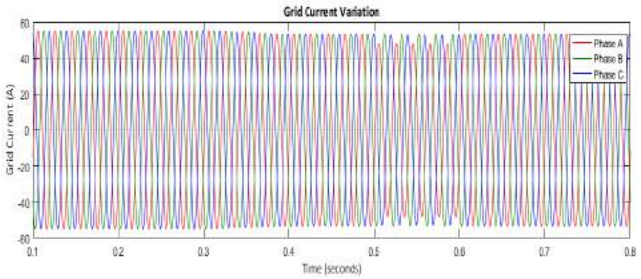

Fig. 7(a). Grid current after harmonic current compensation

Fig. 7(a) presents the waveform of grid current after implementation of the proposed control technique. It can be followed that pure sinusoidal current is obtained at the PCC in presence of nonlinear load and the THD of 3.71% is achieved as in Fig, 7(b) and (c). Hence, the controller is working efficiently under the condition of balanced non-linear load and constant solar irradiance.

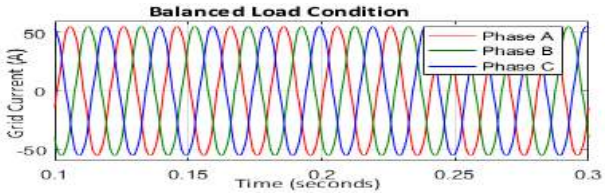

Fig. 7(b). Grid current under balanced load condition

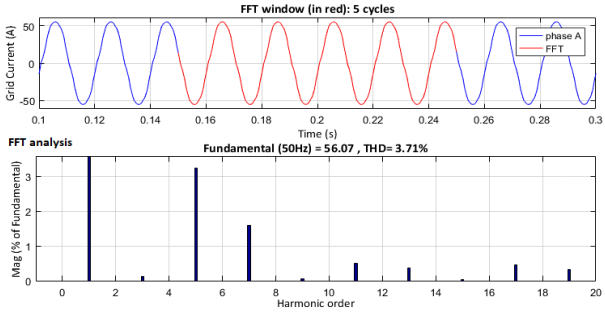

Fig. 7(c). THD of grid current under balanced load condition

After t = 0.3 sec, there is a variation in solar irradiance from 1000 W/m^2 to 800 W/m^2, as a result the contribution of PV towards grid is reduced. However, under dynamic conditon the controller successfully eliminates the nonlinearity from the grid current as shown in Fig. 8(a) and (b).

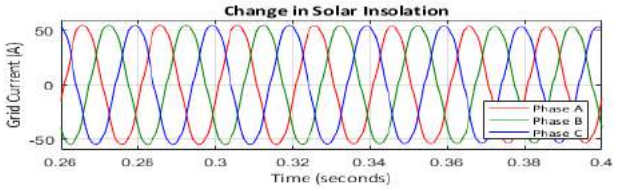

Fig. 8(a). Grid current under varying solar irradiance

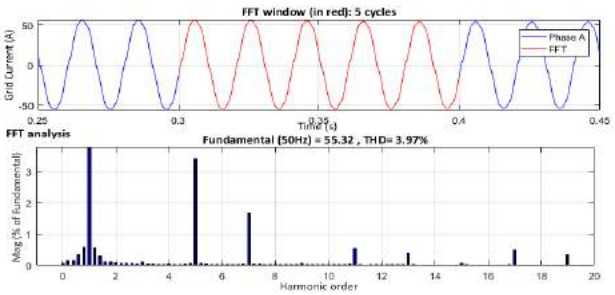

Fig. 8(b). THD of grid current under varying solar irradiance

At t = 0.5 sec, unbalanced load condition is applied and under this condition also the controller is providing harmonic free grid current as presented in Fig. 9(a) and (b)

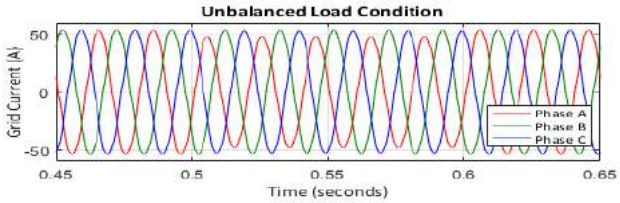

Fig. 9(a). Grid current under unbalanced load

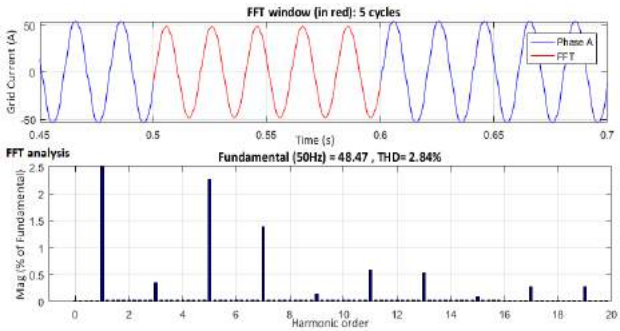

Fig. 9(b). Harmonic content of grid current under unbalanced load condition

The variation of dc link voltage with change in solar insolation and unbalanced load condition is displayed in Fig. 10. It is observed that a constant voltage is maintained around dc link capacitor. When the irradiance changes from 1000 W/m^2 to 800 W/m^2 at t = 0.3 sec, voltage of dc-link is dropped. However, due to the implementation of voltage controller the dc-link voltage changes adaptively. It is also seen that, during unbalanced load condition, dc link voltage is marginally increased which then comes down to its previous constant voltage.

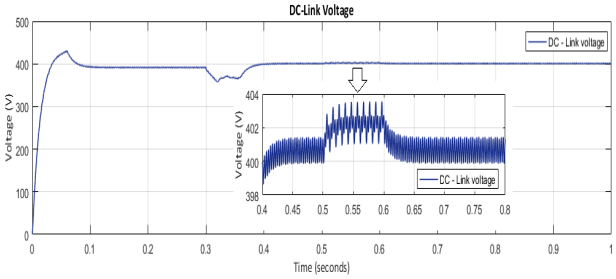

Fig. 10. DC-link voltage

B. *Experimental Result*

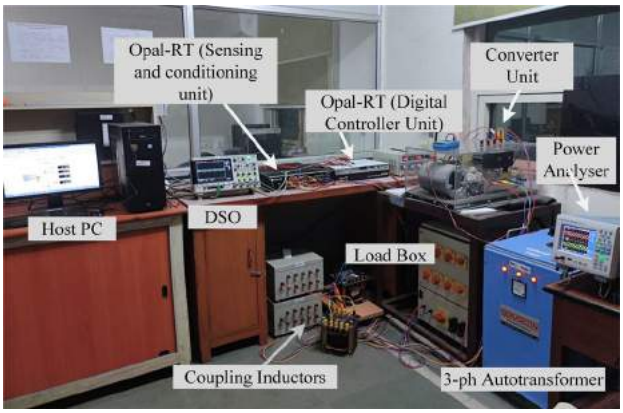

Fig. 11. Experimental prototype of the presented work

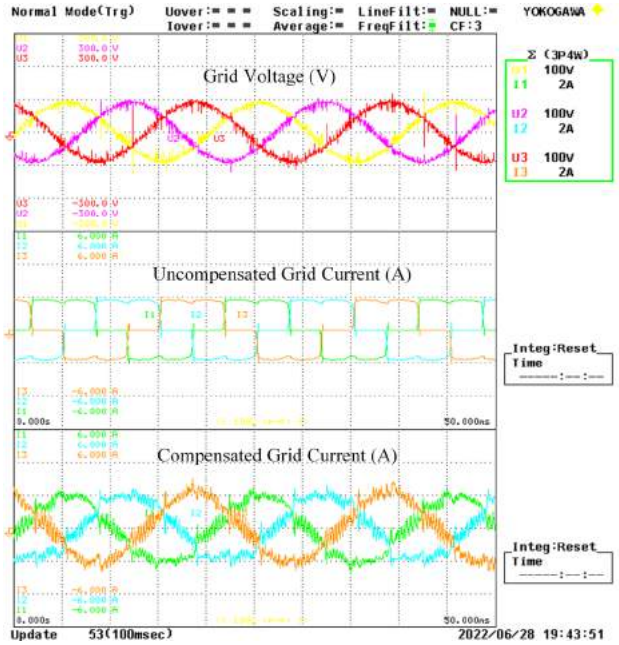

Fig. 12. Experimental setup of the proposed system

The experimental prototype of the presented work is shown in Fig. 11. The parameters required for experimental setup are provided in Table I. Fig. 12 shows that the non-linearity introduced into the grid current is compensated by the proposed controller and sinusoidal waveform is obtained. Fig. 13 depicts the efficient tracking of the voltage of DC-link to attain the desired value of 220 V.

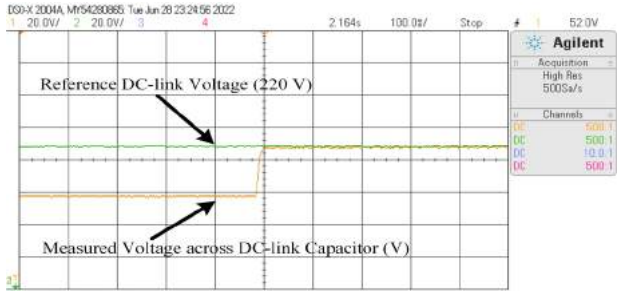

Fig. 13. DC- link voltage tracking performance

TABLE I. SYSTEM PARAMETERS

Parameter	Simulation Value	Experimental value
Grid Line voltage (V_{abc})	415 V, 3-ph 50Hz	100 V, 3-ph 50Hz
DC-link capacitor (C_{dc})	8.5 µF	4.4 µF
Coupling inductor (L_f)	2.5 mH	4.8 mH
Non-linear load	3-ph diode bridge, 14 Ω, 75 mH	Non-linear load drawing 2A current
V_{MPP} and I_{MPP} of PV	726 V and 24 A	240 V and 4.1 A

V. CONCLUSION

A noise-detection based control approach is implemented for VSI's reference current generation. The voltage of dc-link is also adaptively governed to attain its desired value even under sudden changes in the system. From the simulation as well as experimental result it is noticeable that the controller is working properly under all the erratic conditions of varying solar irradiance and load conditions. Further, this work can be utilized to improve both current as well as voltage related power quality issues along with power management by introducing unified power quality conditioner (UPQC).

ACKNOWLEDGEMENT

The authors would like to thank DST, Govt. of India for supporting the research vide no. DST/INT/Thai/P-12/2019

REFERENCES

[1] N. K. Kummari, A. K. Singh and P. Kumar, "Comparative evaluation of DSTATCOM control algorithms for load compensation," in *Harmonics and Quality of Power (ICHQP), 2012 IEEE 15th International Conference*, Hong Kong, China, 2012.

[2] H. Akagi, Y. Kanazawa and A. Nabae, "Generalized Theory of Instantaneous Reactive Power and its Application," *Transaction of the IEEE- Japan,* vol. 103, no. 7, pp. 483-490, 1983. K. Elissa, "Title of paper if known," unpublished.

[3] W. Duesterhoeft, M. W. Schulz and E. Clarke, "Determination of Instantaneous Currents and Voltages by Means of Alpha, Beta, and Zero Components," *Transactions of the American Institute of Electrical Engineers,* vol. 70, no. 2, pp. 1248-1255, July 1951.

[4] B. Singh, C. Jain, S. Goel, R. Gogia and U. Subramaniam, "A Sustainable Solar Photovoltaic Energy System Interfaced with Grid-Tied Voltage Source Converter for Power Quality Improvement," *Indian Academy of Sciences,* vol. 45, no. 2, pp. 171-183, 2017.

[5] R. H. Park, "Two-Reaction Theory of Synchronous Machines: Generalized Method of Analysis - Part I," *Transactions of the AIEE,* vol. 48, pp. 716-730, 1929.

[6] S. Devassy and B. Singh, "Design and Performance Analysis of Three-Phase Solar PV Integrated UPQC," *IEEE Transactions on Industry Applications*, vol. 54, no. 1, pp. 73-81, Jan.-Feb. 2018, doi: 10.1109/TIA.2017.2754983.

[7] L. Chen, A. Amirahmadi, Q. Zhang and N. Kutkul, "Design and implementation of three-phase two stage grid-connected module integrated converter," *IEEE Transactions Power Electron,* vol. 29, no. 8, pp. 3881-3892, 2014.

[8] L. Marco, R. Teodorescu and B. Frede, "Multiple Harmonics Control for Three-Phase Grid Converter Systems With the Use of PI-RES Current controller in a Rotating Frame," *IEEE Transactions on Power Electronics,* vol. 21, no. 3, pp. 836-841, May 2006.

[9] R. Teodorescu, F. Blaabjerg, Liserre and P. Loh, "A New Breed of Proportional-Resonant Controllers and Filters for Grid-Connected Voltage Source Converters," *Proc. OPTIM,* vol. 3, pp. 9-14, 2004.

[10] S. Srikanthan, M. K. Mishra and R. K. V. Rao, "Improved hysteresis current control of three-level inverter for distribution static compensator application," *IET Power Electronics,* vol. 2, no. 5, pp. 1755-4535, 28 August 2009.

[11] B. Singh and C. Jain, "A Decoupled Adaptive Noise Detection Based Control Approach for a Grid Supportive SPV System," *IEEE Transactions on Industry Applications,* vol. 53, no. 5, pp. 4894-4902, September/October 2017.

[12] B. Singh, S. R. Arya and J. Chinmay, "Simple peak detection control algorithm of distribution static compensator for power quality improvement," *IET Power Electronics,* vol. 7, no. 7, pp. 1736-1746, 14 July 2014.

[13] C. Jain and B. Singh, "A Three Phase Grid-Tied SPV System With Adaptive DC Link Voltage for CPI Voltage Variations," *IEEE Transactions on Sustainable Energy,* vol. 7, no. 1, pp. 337-344, January 2016.

[14] B. Singh, C. Jain and S. Goel, "ILST Control Algorithm of Single-Stage Dual Purpose Grid Connected Solar PV System," *IEEE Transactions on Powe Electronics,* vol. 29, no. 10, pp. 5347-5357, October 2014.

[15] N. Femia, G. Petrone, G. Spagnuolo, and M. Vitelli, "Optimization of perturb and observe maximum power point tracking method," *IEEE Trans. Power Electron.*, vol. 20, no. 4, pp. 963–973, Jul. 2005.